Journal of Exposure Science and Environmental Epidemiology (2013) 23, 232–240

www.nature.com/jes

ORIGINAL ARTICLE

Intra-urban spatial variability in wintertime street-level concentrations of multiple combustion-related air pollutants: The New York City Community Air Survey (NYCCAS)

Jane E. Clougherty[1], Iyad Kheirbek[2], Holger M. Eisl[3], Zev Ross[4], Grant Pezeshki[2], John E. Gorczynski[3], Sarah Johnson[2], Steven Markowitz[3], Daniel Kass[2] and Thomas Matte[2]

Although intra-urban air pollution differs by season, few monitoring networks provide adequate geographic density and year-round coverage to fully characterize seasonal patterns. Here, we report winter intra-urban monitoring and land-use regression (LUR) results from the New York City Community Air Survey (NYCCAS). Two-week integrated samples of fine particles ($PM_{2.5}$), black carbon (BC), nitrogen oxides (NO_x) and sulfur dioxide (SO_2) were collected at 155 city-wide street-level locations during winter 2008–2009. Sites were selected using stratified random sampling, randomized across sampling sessions to minimize spatio-temporal confounding. LUR was used to identify GIS-based source indicators associated with higher concentrations. Prediction surfaces were produced using kriging with external drift. Each pollutant varied twofold or more across sites, with higher concentrations near midtown Manhattan. All pollutants were positively correlated, particularly $PM_{2.5}$ and BC (Spearman's $r = 0.84$). Density of oil-burning boilers, total and truck traffic density, and temporality explained 84% of $PM_{2.5}$ variation. Densities of total traffic, truck traffic, oil-burning boilers and industrial space, with temporality, explained 65% of BC variation. Temporality, built space, bus route location, and traffic density described 67% of nitrogen dioxide variation. Residual oil-burning units, nighttime population and temporality explained 77% of SO_2 variation. Spatial variation in combustion-related pollutants in New York City was strongly associated with oil-burning and traffic density. Chronic exposure disparities and unique local sources can be identified through year-round saturation monitoring.

Journal of Exposure Science and Environmental Epidemiology (2013) **23,** 232–240; doi:10.1038/jes.2012.125; published online 30 January 2013

Keywords: land-use regression (LUR); urban air pollution; fine particles ($PM_{2.5}$); black carbon (BC); nitrogen dioxide (NO_2); sulfur dioxide (SO_2)

INTRODUCTION

Growing evidence links intra-urban gradients in combustion-related pollution exposures to adverse health outcomes including cardiovascular and respiratory disease, and mortality.[1–4] Many such studies have used land-use regression (LUR) modeling to estimate exposures at unmonitored locations throughout an urban area, enabling epidemiological analyses across large urban populations.[5] Few LUR studies, however, have examined patterns in a number of combustion-related pollutants at street-level within a concentrated urban area.

Among the most persistent challenges to understanding the health effects of traffic-related air pollution is disentangling the distinct exposure patterns among complex chemical mixtures. Only a few LUR studies have previously compared spatial patterns in, and key predictors of, multiple pollutants,[6–8] although many studies have explored intra-urban spatial variation in a specific traffic-related pollutant, such as nitrogen dioxide (NO_2)[9] or black carbon (BC). In general, studies of fine particulate ($PM_{2.5}$) concentrations have reported lesser intra-urban variability than for EC or NO_2.[6] More generally, examining a wide range of both primary and secondary pollutants, and an array of urban sources (e.g., traffic, diesel traffic, building space heating and industrial boilers) is necessary to elucidate the health and policy implications of intra-urban exposure gradients.

Owing to differences in source activity and meteorology, spatial patterns in intra-urban concentrations may differ substantially both between and within seasons. In New York City (NYC), there is particular interest in wintertime air pollution due to the high prevalence of residual oil-burning units for heating and hot water provision in large buildings. Some recent evidence suggests that particles emitted from residual oil burning (referred to as "residual oil fly ash") may confer distinct health effects relative to particles from other sources.[10–12] Some prior results indicate that the proportion of $PM_{2.5}$ from buildings sources is higher in NYC than in other US cities;[13] thus, there is particular interest in winter season source–concentration relationships, as detailed here.

Most LUR studies have examined variability across broad metropolitan areas, often including urban, suburban and even rural sites,[1] rather than focusing on variation within an urban core. One prior LUR study in NYC, for example, used data from regulatory monitors across 28 urban and suburban counties surrounding

[1]Department of Environmental and Occupational Health, University of Pittsburgh, Graduate School of Public Health, Pittsburgh, Pennsylvania, USA; [2]New York City Department of Health and Mental Hygiene, New York, New York, USA; [3]Center for the Biology of Natural Systems, Queens College, Flushing, New York, USA and [4]ZevRoss Spatial Analysis, Ithaca, New York, USA. Correspondence: Dr. Jane E. Clougherty, Department of Environmental and Occupational Health, University of Pittsburgh, Graduate School of Public Health, Bridgeside Point I 100 Technology Drive, Suite 350, Pittsburgh, PA 15219, USA.
Tel.: +1 412 624 7494. Fax: +1 412 624 3040.
E-mail: jcloughe@pitt.edu
Received 16 December 2011; revised 14 October 2012; accepted 30 October 2012; published online 30 January 2013

NYC.[14] It remains unknown whether metropolitan-scale models capture the exposure variability relevant within the urban core, and how this fine-scale variation may differ by pollutant.

Prior community-based studies in NYC have explored fine-scale exposure variability within neighborhoods of interest.[15] Although useful towards identifying and characterizing sources of concern for public health (e.g., truck traffic), such community-based studies do not enable systematic comparisons across neighborhoods. Systematic data collection across multiple communities is needed to more clearly understand the contribution of pollution exposures to health disparities.

To better characterize spatial variation in multiple combustion-related pollutants, and to identify key local sources across all neighborhoods in all seasons, the New York City Community Air Survey (NYCCAS) employs a spatially saturated year-round intra-urban monitoring network and LUR modeling methods. This article presents concentration measurements, modeling results and predicted city-wide pollution surfaces produced using data from the first winter season, December 2008 through March 2009.

MATERIALS AND METHODS

Study design and evaluation is detailed elsewhere.[16] Here, we briefly summarize methods related to data interpretation and model building. NYCCAS measures multiple pollutants ($PM_{2.5}$ and metal constituents, BC, nitrogen oxides (NO_x), O_3 and sulfur dioxide (SO_2)) throughout four seasons at 155 locations throughout NYC. As a year-round study designed to elucidate season-specific spatial patterns, we perform six 2-week integrated sampling sessions per season. These 2-week integrated samples do not capture diurnal (within-day) variability. We focus on combustion-related pollutants likely to vary within urban areas, potentially explained by local sources (e.g., vehicular traffic, residual fuels), and previously associated with respiratory and/or cardiovascular health.

Monitoring Methods

We collected integrated $PM_{2.5}$ using inertial impaction (Harvard Impactors (HI), Air Diagnostics and Engineering, Harrison, ME, USA). Pump sampling operated simultaneously at 4 l/min for 15 min/h over 14 days, yielding an 84-h integrated sample. Gravimetric analysis was performed on a Metter Toledo microbalance at RTI International Laboratories (Research Triangle Park, NC, USA). BC was estimated using reflectometry of $PM_{2.5}$ filters on an EEL (Incorporating Evans Electroselenium) smoke stain reflectometer (Model 43D, Diffusion Systems, London, UK); absorbance is calculated using a modified ISO method (International Organization for Standardization, ISO 9835: 1993-ambient air — determination of black smoke index). Passive Ogawa samplers provided 2-week integrated samples of NO_2, NO_x and SO_2. Monitors were mounted at 10–12 feet on utility poles, close to the breathing zone but avoiding vandalism or related interference. Deploying at a consistent height enabled comparison of relative concentrations across the city. Instrumentation and laboratory methods are detailed in Matte et al., 2013.

Spatial site allocation. Spatial allocation of sampling sites is detailed in Matte et al., 2013. Briefly, the 150 *distributed* sites are comprised of 120 *systematic* sites selected using random sampling stratified by traffic and buildings density, and 30 *purposeful* sites, selected in consultation with stakeholders, to ensure: (1) variation in source density, (2) good spatial coverage, (3) at least one monitor in every community district, (4) sites near transportation facilities and large sources and (5) at least two public open space sites per borough. Finally, we selected five *reference sites*, one centrally located in each borough, away from local traffic and large buildings. Three reference sites were co-located with Department of Environmental Conservation (DEC) regulatory monitors in the Bronx, Queens and Staten Island, and two in large city parks (i.e., Manhattan Central Park and Brooklyn Prospect Park).

Temporal site allocation. Twenty-five distributed sites were assigned to each of six winter sessions, randomly allocated to minimize spatio-temporal confounding. To ensure good spatial coverage each session, the random allocation of sites to sessions was constrained such that: (1) all four traffic and building density strata are roughly evenly represented each session, (2) all boroughs are sampled each session, with reasonable spatial distribution.

Quality assurance. Detailed descriptions of QA/QC procedures are described elsewhere.[16] Briefly, each session, we deployed three field blanks and two side-by-side active samplers at reference sites. At five sites (two reference and three street-side), we deployed side-by-side passive samplers. Two-week average $PM_{2.5}$ measurements at Bronx Botanical Gardens were compared with the co-located Federal Reference Monitor while NO_2 and SO_2 concentrations measured at Bronx Botanical Gardens and Queens College were compared with 2-week averages from co-located chemilumiscence monitors.

Data Analysis

Temporal variability in pollution concentrations. The city-wide temporal trend in each pollutant, shown reasonably consistent across the five reference monitors (Figure 1) was incorporated into LUR models using the mean reference value as a temporal covariate. We compared results using an alternative temporal adjustment method, wherein concentrations are divided by the mean reference value each session, and the resultant ratio is multiplied by the seasonal reference mean. In sensitivity analyses, LUR models were re-fit predicting these *proportionally adjusted* concentrations (shown in Figure 2); in all cases, the selected spatial covariates were the same, with comparable magnitude and direction of association.

Spatial source covariate creation. Using data from a range of city, state and national sources, we used geographic information systems (GIS) to summarize traffic and land use variables within buffers of 15 different diameters — in 50 m increments from 50 to 500 m, and in 100 m increments from 500 to 1000 m — around monitoring locations.

Data sets included: New York Metropolitan Transportation Council (NYMTC) traffic data, NYC Department of Environmental Protection (DEP) emissions permit data, NYC Department of City Planning Primary Land Use Tax Lot Output (PLUTO) buildings data, LandScan day and nighttime population and the USGS National Land Cover Dataset (NLCD). Elevati on was derived from the National Elevation Dataset (NED) (http://gisdata.usgs.gov). GIS-based source covariates are summarized in Table 1. We consistently used the data set most contemporaneous with the sampling period (2008–2009), and note that most spatial source information (e.g., roadway location) is reasonably stable over time (see Supplementary materials).

We considered site characteristics identified through systematic site surveys completed at deployment and retrieval (e.g., tree leaf density, construction projects on street segment, evidence of smoking (e.g., cigarette butts on ground within 25 feet)). Additional site characteristics were identified through review of aerial photography and analysis of NYC parcel data (i.e., street canyon aspect ratio; presence of an obstruction (i.e., building) between sampling pole and nearest major roadway). All site characteristics were examined both as potential independent predictors of pollution concentrations, and as potential modifiers of source–concentration relationships, as described under model building.

Assessment of outliers. We identified outliers at the 150 distributed sites as observations with absolute concentration values differing by $>3 \times$ SD from the seasonal mean across all distributed sites. Missing and outlier values from distributed sites were not imputed, although covariate selection and model sensitivity were assessed by removing outliers.

To avoid distortion or bias in temporal adjustment, missing and outlier reference values were imputed. We identified outlier reference site values by examining the relationship between concentrations at each reference site and the mean from the other four reference sites, each session. A reference observation was deemed invalid, and a replacement value imputed, if: (1) its concentration was outside the 95% CI of the mean from the other four, and (2) the difference was unidirectional (e.g., the outlier concentration was either higher or lower than all four others) — suggesting unusual short-term activity near the reference site in question. An imputed value for reference site *a* during session 1 is: the average of site *a*'s concentration during sessions 2 through 6, divided (within each session) by the mean for reference site *b* through *e*. This ratio is then multiplied by the average of reference site values *b* through *e* during session 1.

Selection of model-building observations. We selected a random "modeling subset" of 125 (85%) distributed sites (25 purposeful, 100 systematic). Concentrations at the remaining 25 "validation" sites (15%) were compared with model-predicted concentrations in sensitivity analysis, to

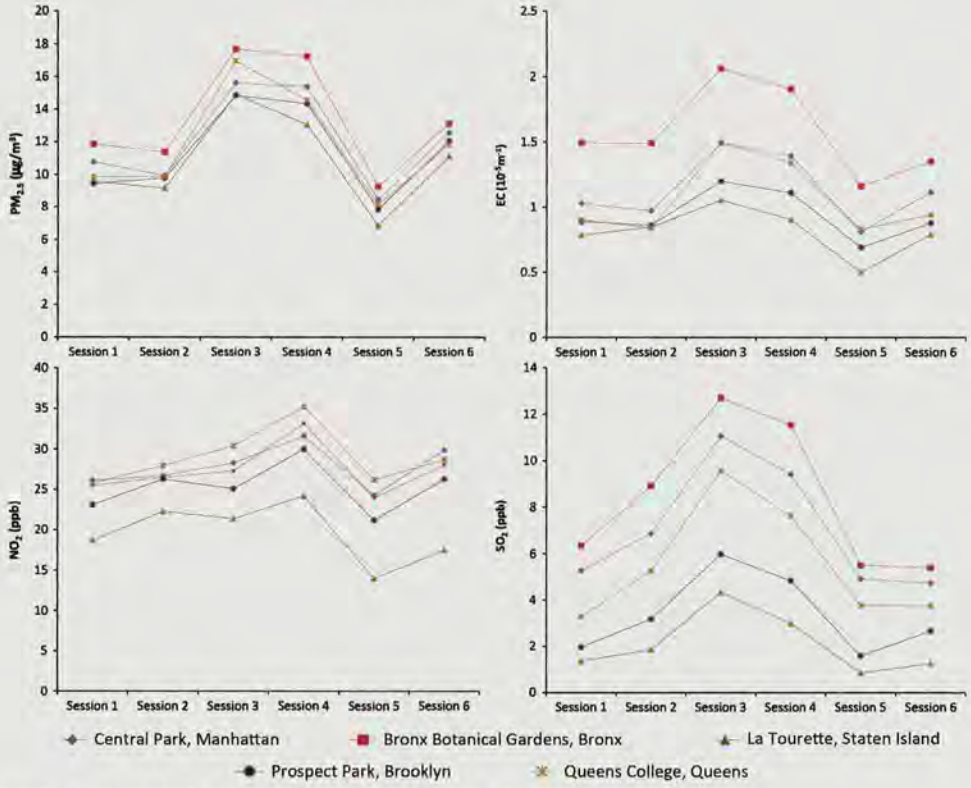

Figure 1. Temporal trends in concentrations across the five reference site monitors.

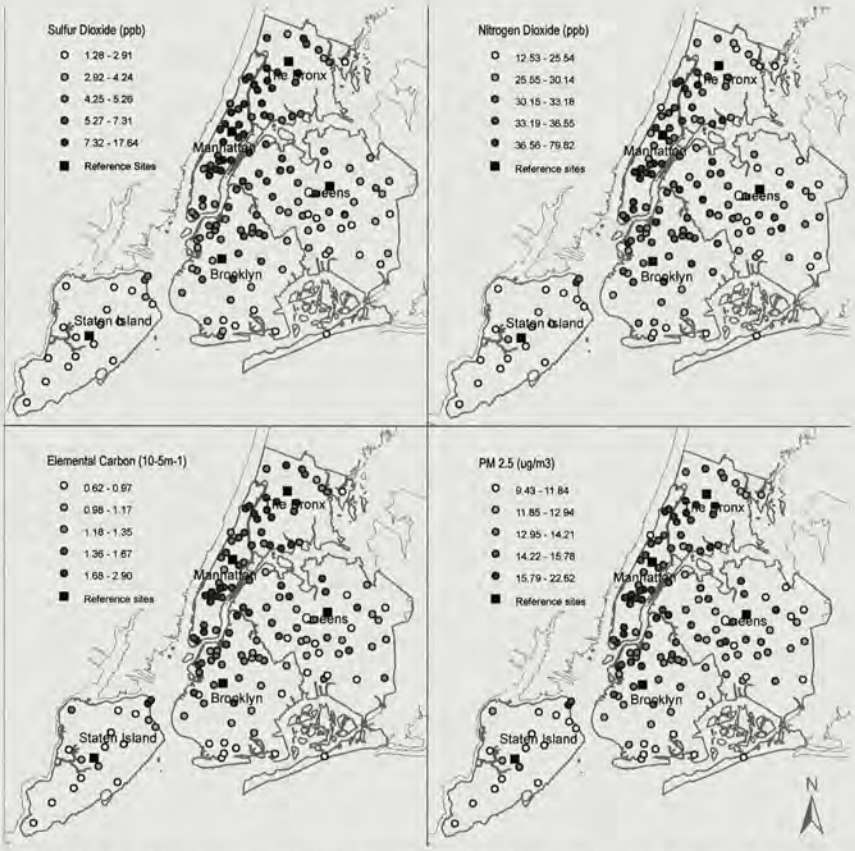

Figure 2. Temporally adjusted concentration measures across the 155 NYCCAS sampling sites, winter 2008–2009.

Table 1. GIS-based source density indicators.

Source category	Variables examined (most calculated in buffers of 50–1000 m)	Data source
Cumulative traffic indicators	Unweighted and kernel-weighted traffic density	New York Metropolitan Transportation Council (NYMTC) traffic data; and US Federal Highway Administration Highway Performance Monitoring System (HPMS) data
	Road density	Accident Location Information System (ALIS) road network data
	Kernel-weighed road density	ALIS network data
	Road density weighted by functional class	ALIS network; MPSI TrafficMetrix data
	Road density kernel weighted by functional class	ALIS network; MPSI TrafficMetrix data
	Number of signaled intersections	NYC Department of Transportation (DOT)
Road-specific measures	Average daily traffic on nearest major road	NYMTC traffic data
	ADT/distance to nearest major road	NYMTC traffic data
	Distance to nearest road, by functional class	ALIS network; MPSI TrafficMetrix data
Truck/diesel-related measures	Unweighted traffic on designated truck routes	NYMTC traffic data
	Unweighted density of truck routes	NYMTC traffic data
	Kernel-weighted density of truck routes	NYMTC traffic data
	Distance to nearest truck route	NYMTC traffic data
	Trucks per day on nearest major road	NYMTC traffic data
Population metrics	Census population density	US Census Bureau 2000 data
	LandScan daytime, nighttime population density	Oak Ridge National Laboratory LandScan data
Built space	Density of built space (building floor area)	NYC Department of City Planning Primary Land Use Tax Lot Output (PLUTO) data
	Density of residential units	PLUTO data
	Total residential, factory, garage floor area	PLUTO data
	Area of commercial floor area	PLUTO data
Land use	Area of industrial and manufacturing	PLUTO data
	Area of heavy manufacturing	PLUTO data
	Area of gas stations	PLUTO data
	Dominant land use type	PLUTO data
Permitted emissions	Number of DEC permitted combustion sources	NYS Department of Environmental Conservation (DEC) permit data
	Number of DEP permitted combustion sources	NYC Department of Environmental Protection (DEP) permit data
	Number of DOB permitted boilers	NYC Department of Buildings (DOB) permit data
	Number of permitted combustion sources by fuel type (oil 2, 4, 6, natural gas)	DEP permit data
	Total BTU by fuel type (oil 2, 4, 6, natural gas)	DEP permit data
	Average BTU by fuel type (oil 2, 4, 6, natural gas)	DEP permit data
Transportation facilities	Number of bus depots	NYC Department of City-Wide Administrative Services (DCAS)
	Minimum distance to bus depot, school bus depot	DCAS; NYC Department of Education (DOE)
	Number of school bus depots	DOE
	Number of school buses at nearest depot	DOE
Distributed facilities	Number of waste transfer stations	NYC Department of Sanitation Inspections (DSNY)
	Minimum distance to waste transfer station, ferry terminal, water treatment facility	DSNY; DCAS
	Distance to nearest port, airport	NYC Office of Emergency Management (OEM)

ensure reasonable predictions. Final model coefficients and smooth surfaces were derived using all sites.

Candidate covariate selection. All GIS-based covariates (Table 1) were grouped into eight categories: (1) total traffic density, (2) roadway lengths and distances to roadway, (3) truck or diesel traffic, (4) population (5) built space, (6) land use and land cover, (7) permitted emissions sources and (8) proximity to transportation facilities and other distributed sources (e.g., distance to airport, waste transfer station).

For each pollutant, we selected the best buffer-specific predictor from a category-specific Pearson correlation matrix including concentrations from all 125 locations in the modeling subset akin to the method described in Su et al., 2009.[17] Supplementary Table II presents the single best buffer-specific bivariate correlations among all screened variables.

A second covariate per category (which best captures concentration variability in combination with the first covariate) was selected using an iterative regression procedure. This iterative procedure individually examined each remaining buffer-specific covariate in the source category, optimizing R^2 in a two-variable model predicting the concentration. This process was repeated using the second-highest Pearson correlation in the matrix, producing a total of four "candidate" covariates per category, considered thereafter in model-building and sensitivity analyses.

LUR model-building process. Using manual forward-stepwise model building and the form in Eq. (1), we built models to predict total concentrations using reference site concentrations and GIS-based source covariates. Model R^2s approximate the total variability explained by temporal and spatial terms; the *spatial* R^2 was produced by predicting temporally adjusted concentrations using the final set of spatial source terms.

$$[\text{Conc}]_{it} = \beta_0 + \beta_1 * \text{Ref}_t + \beta_2 * \text{Source1}_i + \beta_3 * \text{Source1}_i + \beta_4 * \text{Source1}_i * \text{Site\_Characteristic}_{it} + e_{it} \quad (1)$$

$[\text{Conc}]_{it}$ is the measured concentration of the pollutant at location i during sampling period t. Ref_t is the mean concentration of the pollutant across the five reference sites during period t. Source_i is the value of a candidate spatial source term at location i (e.g., traffic density). $\text{Site\_Characteristic}_{it}$ is a non-source site characteristic that may directly influence concentrations, or modify source–concentration associations (e.g., tree density, elevation, street canyon aspect ratio).

Before testing interactions, we sequentially eliminated covariates with $P \geq 0.05$. Thereafter, we required $P < 0.05$ for covariate retention, excepting only main effects for significant interaction terms. LUR models were constructed using Proc Reg or Proc GLM in SAS 9.2.

Ordering of covariate entry into LUR models. We incorporated source categories based on: (1) sampling design, (2) hypothesized sources, (3) correlations with temporally adjusted concentrations, (4) geographic coverage in covariate layers, (5) ordering suggested by automated methods output (tree structures, Random Forest) and (6) interpretability. For pollutants hypothesized to be directly traffic-related (e.g., NO_2, BC), we first considered traffic indicators, then other local source/population terms. For factors hypothesized to be driven primarily by stationary sources (e.g., SO_2, $PM_{2.5}$), we first tested buildings and population terms. Other source categories were incorporated by descending correlation with temporally adjusted concentrations. Within each category, we tested the four candidate covariates; sensitivity analysis for covariate selection using automated methods (e.g., trees, random forest) included all covariates, with no specified entry order.

Forward-stepwise procedure. Using Eq. (1), we first incorporated the mean reference value to account for temporal variation, and then incorporated the source terms from the first category with the strongest univariate correlation with the temporally adjusted pollutant. Source terms were retained if $P < 0.05$, R^2 increased, and variance inflation factor (VIF) < 2.0. We then tested the second-best candidate from the same category, and repeated the process through each source category. Where adding a new term inflated the VIF on an existing term above 2.0, we examined *P*-values, scatterplots and contributions to model fit (sequential R^2) to determine which term to retain.

Finally, we explored effect modification by site characteristics including: street canyon aspect ratio, site characterization as "public open space," percent tree cover, elevation, percent impervious surface (i.e., paved surface or building, *vs* grass) within 100 m.

Examine and map LUR model predictions and residuals. We mapped and examined LUR predictions, residuals and key covariates to identify systematic spatial variation in each. This process identified locations poorly predicted by LUR and suggested overlooked source covariates, which we then created and tested in LUR models (e.g., distance to bus route). Where there was notable spatial variation in model residuals, we re-computed covariate correlation matrices, examining LUR residuals against all covariates, to ensure that significant terms were not overlooked in forward-stepwise procedures. In most cases, residual patterns were not explained by additional GIS terms, and thus were incorporated using kriging with external drift (KED).

Sensitivity testing and LUR model validation. We assessed sensitivity to inclusion of observations using leave-one-out and leave-three-out bootstrapping. Models were validated by predicting concentrations at the 25 withheld validation locations, comparing predicted values with observed concentrations, and evaluating root mean square error, mean absolute percent error (MAPE) and other model diagnostics.

We assessed covariate selection by: (1) removing outliers and influential points, (2) replacing each covariate with others from same source category, (3) replacing significant modifiers to assess uniqueness and interpretability of modification and (4) assessing covariate dependency by individually removing model terms, ensuring all others retain significance.

We assessed sensitivity to model-building procedures using: (1) various temporal adjustment methods, (2) covariates against proportionally adjusted concentrations (approximating percentage of spatial variation explained by model terms) and (3) stepwise backwards elimination, sequentially eliminating the highest *P*-value terms, until all $P < 0.05$.

Kriging with external drift. The unexplained geographic variation was incorporated into the modeling process using KED (also known as "kriging with auxiliary information"), where the "external drift" is represented by the final LUR model. KED is an iterative process wherein residual spatial autocorrelation from an LUR model is fit using a variogram model in *R*.[18] The variogram model is then applied in a generalized least squares model, to account for spatial non-independence in residuals, and LUR parameters are re-estimated.

For presentation purposes, predictions were made on a regular 100 m × 100 m lattice, which was then further smoothed using inverse distance weighting (IDW), allowing influence from the nearest 100 lattice centroids. The IDW was implemented using the Spatial Analyst extension in ArcGIS Desktop 9.2.

Analytical software. Most steps in covariate selection and LUR model building were performed in SAS. Iterative procedures used for sensitivity testing of covariate selection (e.g., tree, RandomForest), variogram fitting, and KED modeling were performed in R version 2.8. Analytic steps related to site selection, covariate creation, review of residual surfaces and final display of predictive maps were performed in ArcGIS Desktop 9.2.

RESULTS

Concentration Data Quality

Wintertime co-located samples for all four pollutants showed excellent reproducibility ($R^2 > 0.96$, MAPE < 6%). At reference sites co-located with DEC regulatory monitors, $PM_{2.5}$ and SO_2 correlations were high ($R^2 > 0.96$) but lower for NO_2 ($R^2 = 0.69$). Lower NO_2 correlations were likely due to limited variability at reference sites during the winter season as the MAPE between measurements showed good comparability (6.8%). Regulatory monitoring data on BC concentrations was not available at these sites. (For more on QA/QC, see Matte et al., this issue). All samplers for all pollutants reported results above the limit of detection and all but one blank (SO_2) showed mass loadings below 5% of average within-session mass loadings.

Concentrations Data Summary

Figure 2 depicts temporally adjusted pollutant concentrations across the 150 distributed sites. Strong spatial variability was observed in all pollutants (Table 2). Unadjusted concentrations ranged 3-fold for $PM_{2.5}$, 5-fold for BC and over 10-fold for NO_2 and SO_2. For all pollutants, concentrations were slightly lower at park sites (including reference sites) than street-side locations.

All four pollutants were across the 150 distributed sites positively correlated, particularly $PM_{2.5}$ and BC (Pearson $r = 0.84$), suggesting common sources. SO_2 was also strongly correlated with $PM_{2.5}$ ($r = 0.70$), and NO_2 with EC ($r = 0.77$). The weakest correlation was between NO_2 and SO_2 ($r = 0.51$) (Table 3).

Modeling Results

Fine particles. $PM_{2.5}$ concentrations were most strongly influenced by temporal variability, indicated by the mean concentration from the five reference sites (Seq $R^2 = 0.61$). One high outlier was removed before LUR model building, after confirming unusual local source activity documented in field surveys. $PM_{2.5}$ spatial variability within the city was most strongly associated with the density of nearby oil-burning units (number 2, 4, or 6 oil). Accounting for other spatially distributed sources, our models indicate that an interquartile range (IQR) increase in the density of oil-burning units within 1 km was associated, on average, with an increase in $PM_{2.5}$ concentrations of 1.65 $\mu g/m^3$ (Table 4). Temporal variability and oil burning, together, explained the majority of variability in $PM_{2.5}$ concentrations (Seq $R^2 = 0.80$ compared with total model R^2 of 0.86). After sensitivity analyses, one traffic covariate was replaced to improve interpretability and model fit. The final model predicted concentrations at validation locations with a MAPE of 9.9% ($R^2 = 0.77$).

As shown in Table 4, traffic density explained additional spatial variability in $PM_{2.5}$; an IQR increase in traffic within 100 m of a sampling site was associated, on average, with an increase in 0.41 $\mu g/m^3$ in $PM_{2.5}$. An IQR increase in truck traffic density within 1 km was associated with 0.75 $\mu g/m^3$ $PM_{2.5}$, and increased Seq R^2 from 0.85 to 0.86. The KED model improved the MAPE by 0.11% over LUR.

Figure 3 depicts predicted wintertime $PM_{2.5}$ concentrations across NYC, derived from LUR and KED. Notably, we observe higher $PM_{2.5}$ in areas of relatively higher buildings and traffic

densities (e.g., midtown Manhattan). $PM_{2.5}$ was also higher along highways and major roads (e.g., in the Bronx), and near clusters of large buildings. The lowest $PM_{2.5}$ concentrations in NYC were observed in the outer boroughs, in locations away from major roads and large buildings.

Black carbon. Temporality accounted for lesser variability in total BC ($R^2 = 0.19$), than for $PM_{2.5}$. Spatial variability in BC was most strongly associated with truck traffic (spatial $R^2 = 0.30$), as a one-IQR increase in truck traffic within 1 km of a sampling site conferred an BC concentration increase in 0.16 absorbance units ($10^{-5}m^{-1}$; Table 4). After sensitivity analyses, one oil-burning covariate was replaced for interpretability, and a redundant nighttime population variable was removed. The final model-predicted concentrations at validation locations with a MAPE of 23.3% ($R^2 = 0.35$).

Oil burning contributed significantly to spatial variation in BC. After adjusting for other sources, an IQR increase in the count of units burning number 2, 4 or 6 fuel oil within 200 m conferred BC concentrations that were 0.21 absorbance units ($10^{-5}m^{-1}$) higher, on average. BC was also associated with traffic density within 100 m, and the density of industrial land use within 1 km (Table 4). KED did not improve MAPE (LUR predictions were 0.22% better).

Predicted BC concentrations (Figure 4) indicate higher wintertime BC concentrations in central-city locations (e.g., Manhattan and the Bronx), where truck traffic, total traffic and fuel-oil burning are higher, relative to other parts of NYC. The lowest BC concentrations were in the outer boroughs, further from dense sources.

Nitrogen dioxide. Temporal variation accounted for lesser variation in NO_2 (Seq $R^2 = 0.16$). Higher NO_2 were closely associated with buildings density — total interior space within 1 km — potentially reflecting emissions from space heating and other sources in and around large buildings (e.g., cooking, idling vehicles). Accounting for other sources, our models indicate that an IQR increase in density of built space was associated with an additional 3.2 p.p.b. NO_2. During sensitivity analysis, we identified higher concentrations along bus routes, and developed and included this term. The final model-predicted concentrations at validation locations with a MAPE of 18.4% ($R^2 = 0.44$), which was not improved using KED (LUR predictions were 0.24% better).

Local traffic density also contributed to city-wide differences in NO_2. At NYCCAS sampling sites located on bus routes, NO_2 concentrations were 4.8 p.p.b. higher, on average, than at other sites, after accounting for temporality, buildings, and kernel-weighted traffic density. An IQR difference in kernel-weighted traffic density within 100 m of the sampling site conferred an average increase in 1.04 p.p.b. in NO_2 (Table 4).

The map in Figure 5 shows estimated city-wide wintertime NO_2 concentrations. Predicted concentrations are generally higher in the denser central parts of the city (e.g., Manhattan). In outer parts of the city, NO_2 was only elevated in areas with a relatively high density of buildings, and along major roadways.

Sulfur dioxide. Unlike other pollutants, SO_2 concentrations at NYCCAS sampling sites were lower, on average, than at the DEC SO_2 regulatory monitors (Figure 2). There are, however, only three DEC SO_2 monitors reporting in NYC, two in areas of the Bronx with higher densities of residual oil boilers than in other parts of the city. SO_2 varied significantly over the winter season (temporal $R^2 = 0.35$).

The spatial pattern in SO_2 was strongly predicted by the number of residual oil-burning units (#4 or #6 oil) within 1 km of the sampling site. An IQR increase in density of oil-burning units conferred an increase in 0.95 p.p.b. in SO_2, on average, in the LUR (Table 4). Note that, because the distribution of SO_2 across sampling sites was highly right-skewed, the IQR difference may under-represent true SO_2 variability across sites. No model improvements were identified through sensitivity analysis. The final model-predicted concentrations at validation locations with a MAPE of 28.1% ($R^2 = 0.76$).

Similarly, areas of higher nighttime population were associated with higher SO_2 concentrations. On average, an IQR increase in residential population density within 1 km predicted an SO_2 increase in 1.61 p.p.b., after accounting for temporality and oil-burning terms. The KED model produced a 0.56% improvement in MAPE, over the LUR.

Figure 6 depicts model-predicted wintertime average SO_2 concentrations across NYC. Concentrations are estimated to be higher in denser parts of the city, with more residual oil-burning units, compared with less dense areas. Unlike the other pollutants, SO_2 was not associated with traffic.

DISCUSSION

The four pollutants reported here — $PM_{2.5}$, NO_2, BC and SO_2 — varied from 2- to 10-fold across city-wide NYCCAS monitoring sites. For three pollutants — $PM_{2.5}$, NO_2 and BC — spatial patterns were explained by a combination of building and traffic-related indicators. Although there were some differences in the spatial patterns, concentrations were generally higher near high concentrations of both traffic and buildings sources — including Manhattan (especially midtown and downtown), and sections of the Bronx, Brooklyn and Queens, along busy freeways. Although concentrations of all pollutants were lowest on average in Staten Island, there were also some high concentrations found there, along highways, and in areas with relatively higher buildings density.

The relationships between air pollutants in NYC and traffic and land use-related covariates were similar to those observed in other

Table 3. Pearson correlations across all four pollutants.

	$PM_{2.5}$	BC	NO_2	SO_2
$PM_{2.5}$	1.0			
BC	0.84	1.0		
NO_2	0.74	0.77	1.0	
SO_2	0.70	0.73	0.51	1.0

Table 2. Summary statistics for raw (unadjusted) wintertime pollutant measurements.

	Reference sites					*Distributed (systematic and purposeful) sites*						
	n	*Mean*	*SD*	*Min*	*Max*	n	*Mean*	*SD*	*Min*	*Max*	*IQR*	*Units*
$PM_{2.5}$	29	12.22	3.04	6.87	17.68	146	14.04	4.03	7.35	26.48	5.69	$\mu g/m^3$
BC	29	1.10	0.35	0.50	2.06	146	1.32	0.46	0.57	2.84	0.57	$10^{-5}m^{-1}$
NO_2	30	25.85	4.49	14.01	35.21	150	32.20	9.86	8.61	84.80	10.02	p.p.b.
SO_2	29	5.32	3.27	0.86	12.71	150	5.36	3.52	0.86	18.95	4.96	p.p.b.

Table 4. Final LUR and KED covariates and model fits for each pollutant.

Covariate description	*B (SE)*	*LUR model*					*KED model*	
		Concentration increase per source IQR	*IQR of source indicator*	*P-value*	*Seq R^{2a}*	*Spatial R^{2b}*	*B (SE)*	*KED model R^{2c}*
$PM_{2.5}$ ($\mu g/m^3$)								
Intercept	−1.45 (0.57)	—		0.01	—	—	−1.70 (0.55)	
Reference site mean ($\mu g/m^3$)	1.08 (0.05)	—		<0.0001	0.61	—	1.11 (0.041)	
Number of oil-burning units (# 2,4,6) within 1 km	0.0055 (5.9×10^{-4})	1.65	310	<0.0001	0.80	0.47	0.0049 (0.00075)	
Kernel-weighted traffic within 100 m (veh-km/h)	0.0047 (0.0009)	0.41	85.1	<0.0001	0.85	0.58	0.0048 (0.00077)	
NYMTC truck traffic within 1 km (veh-km/h)	0.0015 (3.7×10^{-4})	0.75	437.2	<0.0001	0.86	0.62	0.0013 (0.00042)	0.86
BC ($10^{-5} m^{-1}$)								
Intercept	-5.69×10^{-3} (0.12)	—		0.96	—	—	−0.023 (0.11)	
Reference site mean ($10^{-5} m^{-1}$)	0.83 (0.11)	—		<0.0001	0.19	—	0.89 (0.092)	
NYMTC truck traffic within 1 km (veh-km/h)	3.2×10^{-4} (6.5×10^{-5})	0.16	437.2	<0.0001	0.47	0.30	1.83×10^{-4} (7.73×10^{-5})	
Number of oil-burning units (# 2,4,6) within 200 m	0.013 (0.002)	0.21	15.75	<0.0001	0.57	0.43	0.011 (1.91×10^{-3})	
Industrial space within 1 km (km^2)	0.56 (0.14)	0.056	0.102	0.0001	0.62	0.49	0.37 (0.17)	
Kernel-weighted traffic within 100 m (veh-km/h)	5.3×10^{-4} (1.8×10^{-4})	0.046	85.1	0.004	0.65	0.51	6.43×10^{-4} (3.7×10^{-4})	0.60
NO_2 (p.p.b.)								
Intercept	−9.74 (4.54)	—		0.03	—	—	−10.28 (4.19)	
Reference site mean (p.p.b.)	1.34 (0.17)	—		<0.0001	0.16	—	1.32 (0.16)	
Built space within 1 km (km^2)	1.20 (0.09)	3.2	2.62	<0.0001	0.57	0.46	1.14 (0.14)	
Site On a bus route (yes/no)	4.79 (1.05)	NA	NA	<0.0001	0.65	0.56	5.30 (0.95)	
Kernel-weighted traffic within 100 m (veh-km/h)	0.012 (0.004)	1.04	85.1	0.001	0.67	0.59	9.59×10^{-3} (3.24×10^{-3})	0.65
SO_2 (p.p.b.)								
Intercept	−2.30 (0.44)	—		<0.0001	—	—	−2.32 (0.44)	
Reference site mean (p.p.b.)	0.98 (0.068)	—		<0.0001	0.35	—	1.06 (0.064)	
Number of oil-burning units (# 4,6) within 1 km	0.018 (0.002)	0.95	53	<0.0001	0.71	0.53	0.018 (0.00263)	
LandScan nighttime population within 1 km (# persons)	3.6×10^{-5} (5.6×10^{-6})	1.61	43,689	<0.0001	0.77	0.64	3.05×10^{-5} (6.5×10^{-6})	0.77

[a]Seq R^2 is the sequential model fit for each additional term, in a model predicting raw concentrations.
[b]Spatial R^2 is the sequential model fit for each additional term, in a model predicting temporally adjusted concentrations.
[c]R^2 for KED model is approximated using: model sum of squares/total sum of squares.

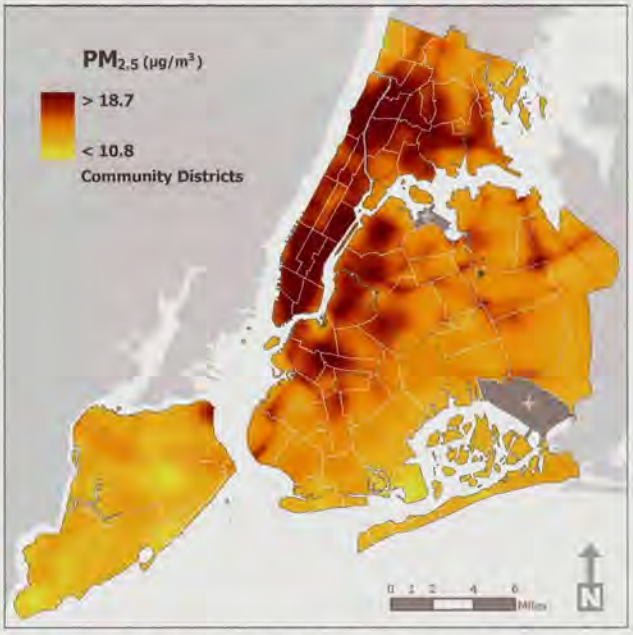

Figure 3. Map of estimated fine particles ($PM_{2.5}$) concentrations, winter 2008–2009.

urban areas. For example, in one of the first LUR studies of urban air pollution, NO_2 concentrations in Amsterdam, Prague and Huddersfield, England, were associated with indicators of nearby traffic and land use, including buildings density.[19] In Munich, estimated annual average $PM_{2.5}$ and BC varied more than twofold across 40 monitoring sites;[20] higher levels were associated with traffic density and population density (potentially linked to buildings-related emissions).[21] NO_2 levels in Toronto were found to be associated with nearby traffic density, nearby dwellings, and industrial land use.[22] Our city-wide model results for BC and NO_2 are consistent with findings from prior studies in specific NYC neighborhoods, which documented higher concentrations of BC and NO_2 in high-traffic areas.[15,23,24]

The geographic pattern in SO_2 differed from those of $PM_{2.5}$, NO_2, and BC. SO_2 was primarily associated with indicators of residual oil (#6 or #4) burning and population density, but not with traffic. This result is in keeping with the higher sulfur content of residual fuel oil, relative to other fuels. The association with population may also partially reflect the use of fuel oil to heat large buildings, an effect that is likely imperfectly captured by the number of permitted units. Large combustion boilers burning residual fuel oil are most concentrated in Manhattan and western Bronx, and in some Brooklyn and Queens neighborhoods. Few prior studies have examined intra-urban variation in SO_2. One study, in Windsor, Ontario linked SO_2 concentrations with dwellings density and SO_2-emitting facilities, a finding that is similar to ours.[5] In Windsor,

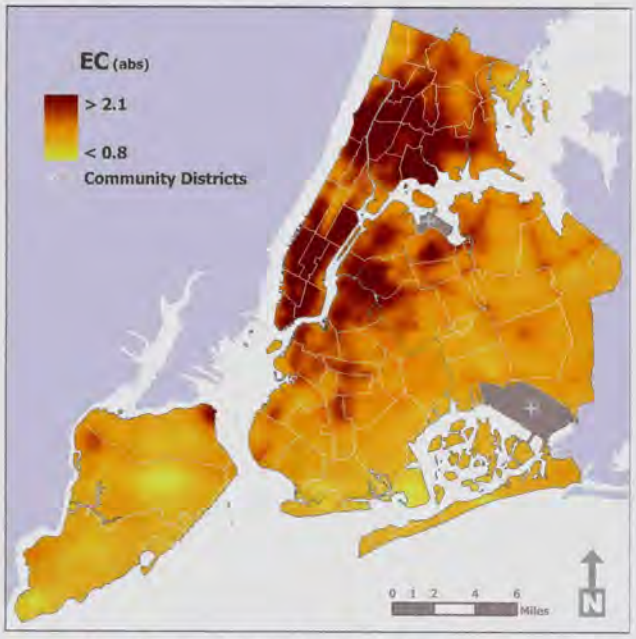

Figure 4. Map of estimated black carbon (BC) concentrations, winter 2008–2009.

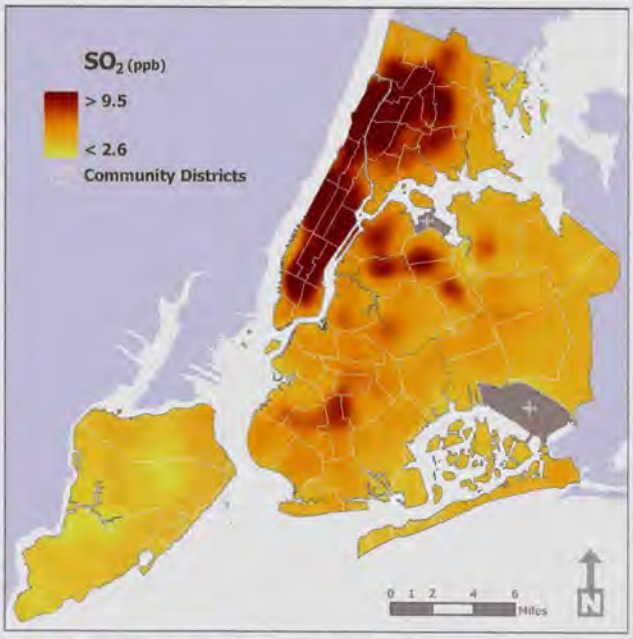

Figure 6. Map of estimated sulfur dioxide (SO_2) concentrations, winter 2008–2009.

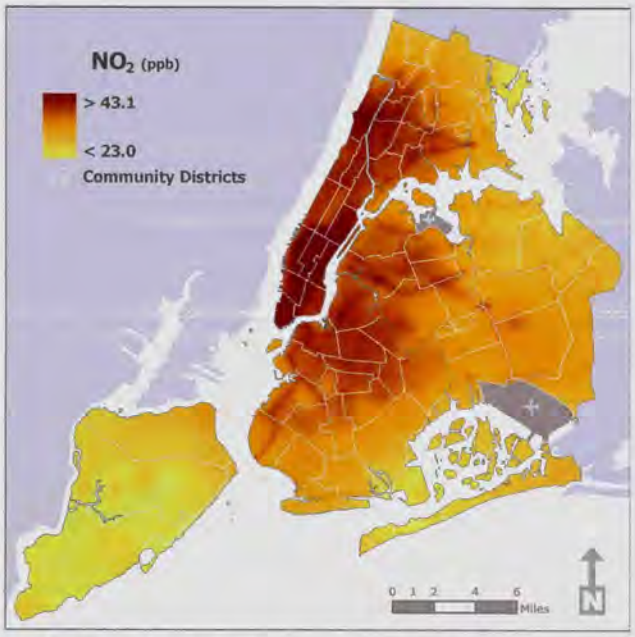

Figure 5. Map of estimated nitrogen dioxide (NO_2) concentrations, winter 2008–2009.

however, SO_2 was also higher near a heavily traveled bridge, whereas we found no independent association between SO_2 and any traffic indicators. The temporal variation we found in SO_2 may indicate uneven residential heating activity during the winter season, which likely varies with temperature.

Site characteristics (e.g., street canyon aspect ratio, tree cover) did not significantly modify source–concentration associations or improve LUR model fits. Future multi-season analyses will further explore such modification as, for example, tree cover may more strongly modify source effects during summer than winter.

A major strength of this monitoring program is the capture of spatial variation in several combustion pollutants in a complex urban environment. The spatial and temporal resolution in our data allows for analysis of sources unevenly distributed within and across seasons, (e.g., heating oil burning). To date, most LUR studies have sought to predict annual average concentrations using spatial source indicators. Fewer have examined spatial patterns separately for each season, or within season. Source activities that vary by season, temperature, or humidity (e.g., space heating) may produce very different exposure patterns, an effect that may be confounded or exacerbated by mixing height or other meteorological effects on dispersion. Characterizing the determinants of spatial variation to individual pollutants, as presented here, provides important data that can guide local policy development, particularly when targeting sources that vary temporally in intensity of impact.

These findings indicate that some NYC neighborhoods may be impacted by high levels of multiple pollutants, because of common sources. High density of oil-burning boilers was found to contribute to higher levels of $PM_{2.5}$, BC and SO_2, pollutants found to correlate well spatially. High-traffic density contributed to higher levels of both $PM_{2.5}$ and NO_2, whereas truck traffic contributed to higher levels of $PM_{2.5}$ and BC, resulting in similar spatial patterns among these pollutants. Evidence from other LUR analyses indicates that traffic density in NYC also contributes to air toxics such as benzene and formaldehyde, increasing the multiple-pollutant exposure burden in these neighborhoods.[25] Future analyses will examine source contributions to multi-pollutant environments using factor analyses of $PM_{2.5}$ constituents and gaseous pollutants, and related methods for modeling multiple pollutants.

These data represent only one winter season, December 2008 through March 2009, and may differ from concentrations in other winters because of weather or other factors. Spatial patterns in air pollution, however, should be relatively consistent from year to year, as the location of major pollution sources, such as highways, are relatively fixed. NYCCAS continues to collect monitoring data over ensuing seasons, enabling comparisons over time into the future.

Our integrated measurements provide no temporal resolution within 2-week sampling period. Thus, we cannot currently disentangle diurnal patterns due to traffic or meteorology and

cannot separate weekday from weekend emissions and pollution patterns. Other limitations include uncertainties in the underlying GIS data layers that may not fully account for pollutant emissions. We have also elected to build models by categorizing source indicators by emitter type, resulting in groupings of multiple highly correlated covariates. As a result, some subjectivity is a part of the model-building process and the presented models may not represent the only applicable LUR model as others could have been built with slightly differing covariates and buffer sizes may provide similar model fit. Nonetheless, the models presented are useful in predicting concentrations at unmonitored locations and identifying predominant sources of spatial variability in pollutant levels in NYC.

Finally, like other LUR studies, ours is not designed to estimate pollution concentrations at a specific site (e.g., a single intersection or residential address). Rather, we have captured broad intra-urban exposure differences attributable to pollution sources distributed city-wide. These major sources (e.g., traffic, truck traffic and buildings) contribute, in varying intensities, to pollution concentrations in every NYC neighborhood.

CONFLICT OF INTEREST

The authors declare no conflict of interest.

ACKNOWLEDGEMENTS

We are very grateful to the many individuals who have contributed to the planning and implementation of NYCCAS, including Janice Kim, Bart Ostro, Michael Jerrett, Jonathan Levy, George Thurston, Patrick Kinney, Michael Brauer, James Bryan Jacobson, Hollie Kitson, Alyssa Benson, Andres Camacho, Jordan Werbe-Fuentes, Jonah Haviland-Markowitz, Rolando Munoz, Anna Tilles, Carter H. Strickland and Kizzy Charles-Guzman. This work was supported by the City of New York Department of Health and Mental Hygiene, and NYC Mayor's Office of Long-Term Planning and Sustainability.

REFERENCES

1 Brunekreef B, Janssen NAH, Hartog J, Harssema H, Knape M, van Vliet P. Air pollution from truck traffic and lung function in children living near motorways. *Epidemiology* 1997; **8**: 298–303.
2 Lindgren A, Björk J, Stroh E, Jakobsson K. Adult asthma and traffic exposure at residential address, workplace address, and self-reported daily time outdoor in traffic: a two-stage case-control study. *BMC Pub H* 2010; **10**: 716.
3 Hoek G, Brunekreef B, Goldbohm S, Fischer P, van den Brandt P. Association between mortality and indicators of traffic-related air pollution in the Netherlands: a cohort study. *Lancet* 2002; **360**: 1203–1209.
4 Pope CA, Ezzati M, Dockery DW. Fine-particulate air pollution and life expectancy in the United States. *New Eng J Med* 2009; **360**: 376–386.
5 Brauer M, Hoek G, Van Vliet P, Meliefste K, Fischer PH, Wijga A *et al.* Air pollution from traffic and the development of respiratory infections and asthmatic and allergic symptoms in children. *Am J Resp Crit Care Med* 2002; **166**: 1092–1098.
6 Hochadel M, Heinrich J, Gehring U, Morgenstern V, Kuhlbusch T, Link E *et al.* Predicting long-term average concentrations of traffic-related air pollutants using GIS-based information. *Atmos Environ* 2006; **40**: 542–553.
7 Wheeler AJ, Smith-Doiron M, Xu X, Gilbert NL, Brook JR. Intra-urban variability of air pollution in Windsor, Ontario—Measurement and modeling for human exposure assessment. *Environ Res* 2008; **106**: 7–16.
8 Clougherty JE, Wright RJ, Baxter LK, Levy JI. Land use regression modeling of intra-urban variability in multiple traffic-related air pollutants. *Environ Health* 2008; **7**: 17.
9 Lebret E, Briggs DJ, Collins S, van Reeuwijk H, Fischer P, Smallbone K *et al.* Small area variations in ambient NO2 concentrations in four European areas. *Atmos Environ* 2000; **34**: 177–185.
10 Bell ML, Ebisu K, Peng RD, Samet JM, Dominici F. Hospital admissions and chemical composition of fine particle air pollution. *Am J Resp Crit Care Med* 2009; **179**: 1115–1120.
11 Patel MM, Hoepner L, Garfinkel R, Chillrud S, Reyes A, Quinn JW *et al.* Ambient metals, elemental carbon, and wheeze and cough in New York City children through age 24 months. *Am J Resp Crit Care Med* 2009; **180**: 1107–1113.
12 Roberts JR, Young S-H, Castranova V, Antonini JM. The soluble nickel component of residual oil fly ash alters pulmonary host defense in rats. *J Immunotoxicol* 2009; **6**: 49–61.
13 Qin YJ, Kim E, Hopke PK. The concentrations and sources of PM2.5 in metropolitan New York City. *Atmos Environ* 2006; **40**: S312–S332.
14 Ross Z, Jerrett M, Ito K, Tempalski B, Thurston GD. A land use regression for predicting fine particulate matter concentrations in the New York City region. *Atmos Environ* 2007; **41**: 2255–2269.
15 Kinney PL, Aggarwal M, Northridge ME, Janssen NAH, Shepard P. Airborne concentrations of PM2.5 and diesel exhaust particles on Harlem Sidewalks: a community-based pilot study. *Environ Health Perspect* 2000; **108**: 213–218.
16 Matte TD, Ross Z, Kheirbek I, Eisl H, Johnson S, Gorczynski JE *et al.* Monitoring intra-urban spatial patterns of multiple combustion air pollutants in New York City: Design and Implementation. *J Expo Sci Environ Epidemiol.* advance online publication 16 January 2013.
17 Su JG, Jerrett M, Beckerman B. A distance-decay variable selection strategy for land use regression modeling of ambient air pollution exposures. *Sci Tot Environ* 2009; **407**: 3890–3898.
18 Pearce JL, Rathbun SL, Aguilar-Villalobos M, Naeher LP. Characterizing the spatiotemporal variability of PM2.5 in Cusco, Peru using kriging with external drift. *Atmos Environ* 2009; **43**: 2060–2069.
19 Briggs DJ, Collins S, Elliott P, Fischer P, Kingham S, Lebret E *et al.* Mapping urban air pollution using GIS: a regression-based approach. *Int J GIS* 1997; **11**: 699–718.
20 Cyrys J, Heinrich J, Hoek G, Meliefste K, Lewne M, Gehring U *et al.* Comparison between different traffic-related particle indicators: elemental carbon (EC), PM2.5 mass, and absorbance. *J Expo Anal Environ Epidemiol* 2003; **13**: 134–143.
21 Brauer M, Hoek G, Van Vliet P, Meliefste K, Fischer P, Gehring U *et al.* Estimating long-term average particulate air pollution concentrations: application of traffic indicators and geographic information systems. *Epidemiology* 2003; **14**: 228–239.
22 Jerrett M, Arain MA, Kanaroglou P, Beckerman B, Crouse D, Gilbert NL *et al.* Modeling the intraurban variability of ambient traffic pollution in Toronto, Canada. *J Toxicol Environ Health A* 2007; **70**: 200–212.
23 Lena TS, Ochieng V, Carter M, Holguin-Veras J, Kinney PL. Elemental carbon and PM2.5 levels in an urban community heavily impacted by truck traffic. *Environ Health Perspect* 2002; **110**: 1009–1015.
24 Maciejczyk PB, Offenberg JH, Clemente J, Blaustein M, Thurston GD, Chen LC. Ambient pollutant concentrations measured by a mobile laboratory in South Bronx, NY. *Atmos Environ* 2004; **38**: 5283–5294.
25 Kheirbek I, Johnson S, Ross Z, Pezeshki G, Ito K, Eisl H *et al.* Spatial variability in levels of benzene, formaldehyde, and total benzene, toluene, ethylbenzene and xylenes in New York City: a land-use regression study. *Environ Health* 2012; **11**: 51.

Supplementary Information accompanies the paper on the Journal of Exposure Science and Environmental Epidemiology website (http://www.nature.com/jes)